Space charge measurement in polymer insulated power cables using flat ground electrode PEA system

M. Fu and G. Chen

Abstract: Data processing methods used to accurately determine the space charge and electric stress distributions in DC power cables using the pulsed electroacoustic (PEA) system are described. Due to the coaxial geometry and the thick-walled insulation of high-voltage cables, factors such as divergence, attenuation and dispersion of the propagated acoustic pressure wave in the PEA can strongly influence the resultant measurements. These factors are taken into account ensuring accurate measurements to be made. Most importantly, a method is presented to determine the electric stress profile across the insulation due to both the divergent applied field and that as a consequence of trapped charge in the bulk of the insulating material. Results of space-charge measurements and the corresponding derived electric stress distributions in XLPE DC cables are presented.

1 Introduction

Nowadays a considerable amount of transmission and distribution of electricity, especially in urban areas, is carried out by means of underground power cables. Growing public awareness of environment issues and the need to maintain a highly reliable system has led to polymeric materials progressively replacing oil-impregnated paper insulation in underground cables. Moreover, with large energy pools and separate load centres, reactive power control is difficult. High-voltage direct-current (HVDC) transmission links with their inherent VAr and fault current control capabilities is an attractive option. This renewed interest in HVDC has led to many manufacturers world-wide investing in DC polymeric power cable development.

The electrical properties of insulating materials, such as conduction and breakdown, are strongly affected by the presence of space charge in the bulk of the material. This is particularly true when the dielectric is subjected to a DC stress. If space charge is formed in the extruded insulation of a polymeric power cable, the electric stress distribution may be greatly distorted. This can result in localised electric stress enhancement leading to premature failure of the cable at stresses well below the anticipated or designed values. Prediction by conventional numerical techniques (e.g. finite element) of trapped charge and subsequent stress distributions give only limited information. Models of charge mobility, transportation and trapping phenomena have also been established [1] but lack information on realistic parameters. Therefore there is a need for a better understanding of charge formation in polymeric materials under high-level DC electric stresses and in particular, in the characteristics of charge formation, such as the magnitude and type, its mobility and location in the bulk of the material.

In this paper, a modified PEA system that utilises a flat electrode instead of the curved one [2–4] is briefly introduced. With the use of the flat electrode, the measurements in power cables of various diameters are allowed while maintaining the same detection sensitivity as the curved electrode [5]. However, with a thick insulation as with high-voltage power cables the attenuation and dispersion of the acoustic wave during propagation through the insulation are no longer negligible. Moreover, in the coaxial geometry, the divergence of the pulsed electric stress across the insulation and the divergence of the acoustic wave travelling across the cable insulation may also be significant. A data processing approach was developed to take into account these effects in the original output waveform from the PEA enabling the true space charge distribution to be found. Emphasis has also been placed on quantitative appraisal of the electric stress profile across the insulation allowing for both the divergent field due to the applied voltage and that due to space charge accumulation in the insulation. Results of the space charge and stress distribution for a commercial XLPE cable operating under DC conditions are also presented.

2 Measuring system

2.1 Basic principle of PEA

The PEA technique was developed in 1981[6] to measure the space charge profile in dielectrics. Since then it has become one of the most widely used techniques by researchers from industry and academia. A detailed description of the principles of the method is given elsewhere [7] and only a brief overview is given in this paper.

Consider a plaque sample as shown in Fig. 1 with a space charge layer q_2, which will produce image charge q_1 and q_3 on the electrodes ($q_1+q_3=q_2$). An external voltage pulse $v_p(t)$ is applied producing an electric stress $e_p(t)$ which will introduce a perturbation force p_1, p_2 and p_3 on each charge layer according to Lorentz's law. These forces cause charges

IEE Proceedings online no. *20030225*

doi:10.1049/ip-smt:20030225

Paper first received 29th November 2002 and in revised form 10th January 2003

The authors are with the Department of Electronics and Computer Science, University of Southampton, Highfield, Southampton SO17 1BJ, UK

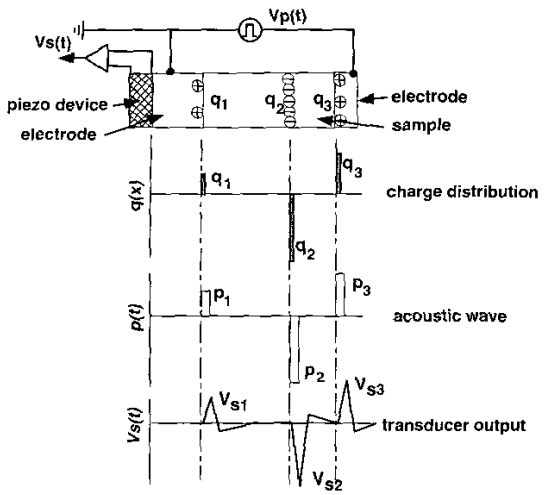

Fig. 1 *Basic principle of PEA method*

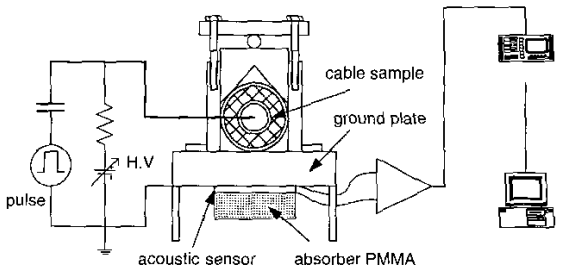

Fig. 2 *Schematic diagram of modified cable PEA system*

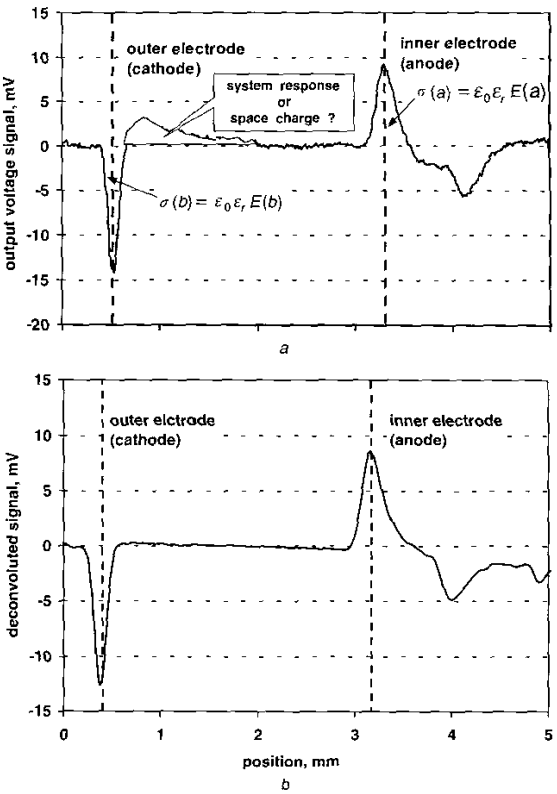

Fig. 3 *PEA output signal*
a Typical output waveform from PEA
b After using a deconvolution method

to move slightly, resulting in acoustic pressure waves that are proportional to the charge magnitudes. A piezoelectric transducer detects the acoustic pressure waves and converts them into electrical signals v_{s1}, v_{s2} and v_{s3}. Measurement of the time-dependent voltage enables a profile to be obtained which is related to the amplitude of the space charge coincident with the propagating acoustic pulse.

2.2 PEA for cable geometry

A considerable amount of work using the PEA technique has been carried out on plaque samples giving invaluable information about space charge formation and trapping. Measurements on coaxial power cables on the other hand, have received comparatively little attention [2–4, 8–11]. Without exception, all studies to date on cable configurations use a ground electrode, sensor and absorber block shaped to fit around the outer diameter of the cable. The limitation of this arrangement is that only one diameter cable can be measured for a particular electrode size. Care has to be taken in assembling the apparatus making sure that a good acoustic contact is made between the cable and curved electrode. Otherwise, mismatching occurs resulting in spurious signals, which can cause incorrect interpretation of the output from the PEA. A modified structure as shown in Fig. 2, adopting a flat ground electrode, has enabled the previously mentioned weaknesses to be overcome. Further details of the arrangement are given elsewhere [12].

The outer semiconducting screens at the two ends of the cable sample are sufficiently stripped back and removed to ensure that the high voltage can be applied to the cable without surface flashover, the remaining section of semiconducting layer is part of the outer earthed electrode. Stress relief rings are also built at the screen cuts to reduce the possibility of failure of the insulation over long term testing of the cable sample.

3 Data processing

3.1 Deconvolution of the raw data

A typical output waveform from the device with a DC voltage applied and assuming it is devoid of any space charge except for the surface charges (indicated by the voltage peaks) on the electrode/sample interfaces is shown in Fig. 3*a*. Any space charge in the bulk would alter the voltage peaks and give rise to voltages at the positions of trapped charge shown as the shaded part in Fig. 3*a*. However, in some cases the frequency response of the transducer and amplifier can cause distortion of the output signal, which can be wrongly interpreted as space charge resulting in a similar waveform to that in Fig. 3*a*. To remove this effect, a deconvolution technique has to be employed to restore the original signal [7, 13].

Fig. 3*b* shows the output signal with the removal of the distortion due to the system response and represents the charge at the interfaces due to the applied voltage across the cable insulation. The small peak to the right hand of the voltage peak at the inner electrode is caused by the acoustic wave reflection at the interface of the inner semiconducting layer and the conductor.

3.2 Geometrical factor correction

3.2.1 Divergence of pulsed electric stress: Unlike the plaque samples where a uniform electric stress distribution is assumed for the external pulse voltage, for the cable geometry the electric stress e_p is given by the

following

$$e_p(t,r) = \frac{v_p(t)}{r \ln(b/a)} \tag{1}$$

where a and b are the inner and outer radii of the insulation respectively and $v_p(t)$ the external pulse voltage. The PEA relies on the interaction between the pulsed electric stress and the charge layer to launch a perturbation force. As a consequence of the nonuniform distribution, the intensity of the acoustic pressure wave initiated from the interaction will depend not only on the charge density but also on the position. Thus the divergent distribution of the pulse stress needs to be taken into account when a quantitative appraisal of the space charge distribution in cable samples is required.

3.2.2 Divergence of acoustic wave propagation in radial direction: For simplicity, it is assumed that the length of the cable sample is much greater than the insulation thickness and the material along the axial direction is homogeneous. The space charge distribution in a coaxial geometry only changes in the radial direction along which the external electric field is applied. Therefore the acoustic pressure wave representing the space charge density variation in this direction is also a one-dimensional distribution and is a radial-position-dependent function. In this case the wave equation can be expressed in cylindrical co-ordinates as [14]

$$\frac{1}{u_{sa}^2}\frac{\partial^2\phi(t,r)}{\partial t^2} = \frac{\partial^2\phi(t,r)}{\partial r^2} + \frac{1}{r}\frac{\partial\phi(t,r)}{\partial r} \tag{2}$$

where $\phi(t, r)$ is the velocity potential of vibration in the medium, and u_{sa} is the velocity of the acoustic wave propagation in the cable insulation. The solution of (2) is

$$\phi(r,t) = \frac{A}{\sqrt{r}} e^{j\left(\frac{\omega}{u_{sa}}r - \omega t\right)} \tag{3}$$

where $k = \omega/u_{sa}$, the wave number, therefore

$$\phi(t,r) = \frac{A}{\sqrt{r}} e^{jk(r-u_{sa}t)} \tag{4}$$

where ω is the angle frequency of the acoustic wave $\omega = 2\pi f$, and A is a constant determined by the boundary conditions. Thus, the pressure wave per unit area at position r is expressed as [14]

$$p(t,r) = \gamma\frac{\partial\phi(t,r)}{\partial t} = -\frac{j\gamma u_{sa}Ak}{\sqrt{r}} e^{jk(r-u_{sa}t)} \tag{5}$$

where γ is the density of medium in which the acoustic wave is launched and travels. This equation describes the propagation of acoustic wave in an elastic (or lossless) medium in the radial direction within a cylindrical co-ordinate system. According to this equation, the intensity of the pressure wave generated by the space charge layer inside the cable insulation will decrease along the radial direction. This factor or ratio can be best described by

$$\frac{p(t+\Delta t, b)}{p(t,r)} = (r/b)^{1/2} \tag{6}$$

where $p(t, r)$ and $p(t+\Delta t, b)$ are the acoustic pressure wave intensities produced at radius r and detected at the outer sheath b after transmission through the insulation, Δt is the time for the acoustic pulse travelling from position r to b. Any divergence in the outer semiconducting layer is neglected.

3.2.3 Correction for geometric divergence: Divergent effects due to cable geometry can be easily explained in the following way. Assuming that there are two charge layers with the same densities at the inner and outer insulation/electrode interfaces, the acoustic pressure produced at the inner interface will be (b/a) times greater than that at the outer interface because of the divergent distribution of the pulse electric stress. Moreover, the detected pressure wave at the outer interface, originating from the inner interface, becomes $(a/b)^{1/2}$ times less owing to acoustic transmission divergence. So the resultant effect of the two factors will falsify the charge density at the inner interface by $(b/a)^{1/2}$ times greater than that at the outer interface. For a cable with its outer radius of insulation being twice the size as the inner radius, the possible difference introduced can be as high as 40% ($(b/a)^{1/2} \approx 1.4$). Therefore these factors must be taken into account if an accurate space charge profile is required. Practically, the signal after the deconvolution is corrected by the geometry factor $(b/r)^{1/2}$.

3.3 Attenuation and dispersion compensation of propagated acoustic wave

For a cable sample, the pressure wave produced by a space charge layer at the inner conductor will be considerably attenuated in magnitude and its shape altered as it travels through the dielectric material to the outer screen. In a lossy and dispersive medium, *i.e.* a polymer, the higher frequency components of the acoustic wave will attenuate and disperse to a greater extent than the lower frequencies. This results in a decrease and broadening of the peak voltage output from the piezoelectric transducer.

Assume a plane pressure wave propagates through a solid specimen and its wave solution in an ideal medium is given as

$$p(tx) = p_0 e^{j(\omega t - kx)} \tag{7}$$

For an ideal medium the pressure wave velocity u_{sa} is a constant and k a real number. In a real system, *e.g.* a lossy and dispersive medium, it is suffice to replace the wave number k by its complex generalisation $k(j\omega)$ [15], where $k(j\omega) = \beta(\omega) - j\alpha(\omega)$, yielding the wave propagation in a viscoelastic medium

$$p(t,x) = p_0 e^{j[\omega t - k(j\omega)x]} = p_0 e^{-\alpha x} e^{j(\omega t - \beta x)} \tag{8}$$

$\alpha(\omega)$ and $\beta(\omega)$ are defined as attenuation and dispersion factors and are the functions of ω. It is seen that the plane-wave intensity decreases ($x>0$, $\alpha>0$) during its propagation. The decay rate is frequency dependent and governed by the imaginary part of the wave number $\alpha(\omega)$. Now the wave velocity is given by

$$u_{sa}(\omega) = \omega/\beta(\omega) \tag{9}$$

thus the velocity is also frequency dependent and governed by the real part of the complex wave number. In other words, in a lossy and dispersive system the acoustic pulse decreases in magnitude due to the attenuation and is broadened since the different harmonic components propagate at different velocities.

Using the Fourier transform, for a coaxial cable geometry (8) is transformed into

$$P(\omega, r) = P(\omega, a)e^{-\alpha(\omega)(r-a)}e^{-j\beta(\omega)(r-a)} \tag{10}$$

where $P(\omega,a)$ and $P(\omega,r)$ are the Fourier transforms of the acoustic wave at a and r, respectively. r varies from a to b. From (10) the attenuation and dispersion factors can be determined by the given acoustic wave profile at two known positions, *e.g.* at the inner ($r=a$) and the outer ($r=b$) insulation/electrode interfaces of the cable insulation. However, the magnitudes of the two induced charges at

interfaces are (assuming no space charge in the bulk) proportional to the applied electric stress. Considering the geometric divergence of the externally applied DC stress, which will be discussed in the following Section, the pressure wave intensity at the outer interface is $\sqrt{a/b}$ times of that at the inner interface. Therefore this ratio has to be taken into account for the acoustic wave initiated from the inner surface charge layer. The attenuation and dispersion factors are determined from the following equations:

$$\alpha(\omega) = -\frac{1}{b-a}\ln\left|\frac{P(\omega,b)}{P(\omega,a) * \sqrt{a/b}}\right| \tag{11}$$

$$\beta(\omega) = \frac{1}{b-a}|\phi(\omega,b) - \phi(\omega,a)| \tag{12}$$

Hence, the transfer function of the acoustic wave through the cable insulation is

$$G(\omega,r) = \frac{P(\omega,r)}{P(\omega,a)} = e^{-[\alpha(\omega)+j\beta(\omega)](r-a)} \tag{13}$$

This transfer function is used in the frequency domain to compensate for the attenuation and dispersion during the acoustic propagation at various positions of r. Thus the actual acoustic pressure profile along the cable insulation may be obtained by the inverse Fourier transform.

Fig. 4 shows the resultant signal before and after the attenuation and dispersion compensation. Two peaks, which are selected between the two pairs of vertical cursors in Fig. 4*a*, are used to calculate the attenuation and dispersion factors. Fig. 4*b* shows the space charge distribution for the given applied voltage after the attenuation and dispersion correction factors have been applied. The amplitudes of the two peaks now are consistent with the externally applied interfacial electric stresses.

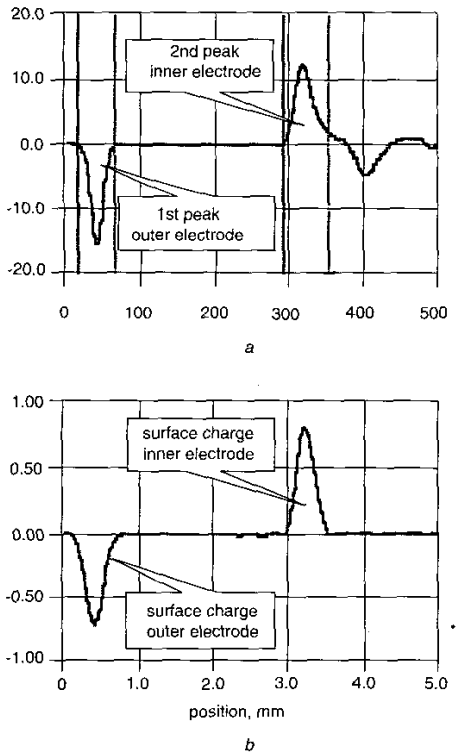

Fig. 4 *Signals before and after propagation compensation*
a Deconvoluted signal
b Recovered signal (calibrated to charge density)

4 Interfacial stress used for space charge density calibration

As the PEA technique is an indirect method of the measurement of the space charge distribution in the dielectric material, the relationship between the piezoelectric transducer output and the charge density has to be determined using a calibration procedure. A sufficiently low voltage is applied across the cable insulation for a short period of time which ensures no space charge is developed in the insulating bulk. The only charge present is the induced surface charge at the inner and outer insulating/electrode interfaces due to the applied voltage across the insulation, as shown in Fig. 3*b*. The induced charge at the inner and outer electrodes is directed proportional to the electric stress at the interface, *i.e.*

$$\sigma(a) = \varepsilon_0\varepsilon_r E(a) \tag{14}$$

$$\sigma(b) = \varepsilon_0\varepsilon_r E(b) \tag{15}$$

where ε_0 is the permittivity of free space, ε_r the relative permittivity of the insulating material, $E(a)$ and $E(b)$ the electric stresses at the two interfaces, respectively. For a fixed pulse voltage and for a given material, the peak height or the area under each peak of the electrical output signal from the PEA system is proportional to the charge density at the electrodes. Knowing the actual charge density at a given interface, the constant of proportionality between the output of the PEA system and charge density can be determined.

It is known that the electric field distribution in an AC cable is dependent on the capacitance (or permittivity), while in DC cables is governed by the conductivity of the insulating material. The variation of dielectric permittivity with either the temperature or electric stress is normally insignificant. In contrast, the conductivity is dependent on the temperature and to a lesser degree the electric stress. The reason for these dependences is still not fully understood and information is of an empirical basis and no physical interpretation is available. Thus it is difficult to predict the electric stress distribution across the cable insulation under DC conditions with the accuracy that can be achieved for AC cables [16]. As a result of the conductivity dependence with temperature and electric stress, in a fully loaded DC power cable, the maximum electric stress will be at the outer semiconducting screen rather than at the conductor. Even without the temperature gradient across the cable insulation, as is the case with the present study which is being carried out at ambient temperature, the electric stress may also be influenced to an unknown extent by the non-uniformly distributed electric stress itself in the coaxial geometry due to field dependent conductivity σ. These characteristics, mainly limited to the oil–paper insulation, had been qualitatively analysed or described by an empirical formulae [16–20]. Studies to date reveal that data on the DC electric stress distribution in polymer-insulated power cables are very limited. It has been reported [21–24] that the conductivity in polymeric materials can be expressed empirically as

$$\sigma = \sigma_0 e^{\alpha T} E^p \tag{16}$$

σ_0 is the conductivity of dielectric material at reference temperature, α and p are the temperature and electric stress coefficients of the material, T is the temperature and E is the electric stress. The derived electric stress at a distance r from the centre of a cable conductor is given by

$$E(r) = \frac{\delta r^{(\delta-1)} U}{b^\delta - a^\delta} \tag{17}$$

where δ is a constant and is determined by the material and the temperature difference across the cable insulation. U is the applied voltage. However, the constant δ in (17) given by Liu [21] and McAllister [23, 24] is 2/3 and that by Tanaka [22], 1/2 for XLPE without a temperature gradient. Consequently the electric stress profiles obtained for these two δ values are significantly different. The ratio between the electric stress at the inner and outer electrode will be $(b/a)^{1/3}$ and $(b/a)^{1/2}$, respectively. It means that using 2/3 as suggested by Liu and McAllister will give a more evenly distributed electric stress across the cable insulation. As a result the calibrated space charges at the inner and outer electrode interface become closer in magnitude [25]. Obviously they both differ from the normal electric stress distribution derived for the AC case, *i.e.*

$$E(r) = \frac{U}{r \ln(b/a)} \tag{18}$$

No matter which expression, (17) or (18), is used, the effect of the electric stress on the insulating material conductivity, the electric stress distribution in DC cable tends to be more uniform across the insulation. This is a favourable condition for DC cable design. However, the issue here is what value is used for the interface stress to determine the charge density in the calibration procedure. In view of the complexity of the problem, the method (or δ value) suggested by Tanaka *et al* [22] has been adopted in this paper to calculation the electric stress distribution in the polymer insulation of a DC power cables when it is void of space charge. Thus the electric stress at the outer electrode/insulation interface is calculated from

$$E(b) = \frac{U}{2\sqrt{b}(\sqrt{b} - \sqrt{a})} \tag{19}$$

The attraction of using the electric stress at the outer electrode is that a relatively small amount of attenuation and dispersion of the acoustic wave occurs at this point. Similarly, the stress at the inner semiconducting layer surface has the form of

$$E(a) = \frac{U}{2\sqrt{a}(\sqrt{b} - \sqrt{a})} \tag{20}$$

and

$$E(b)/E(a) = \sqrt{a/b} \tag{21}$$

Therefore, the factor $\sqrt{a/b}$ is used in (11) to correct for the attenuation of the acoustic signal through the insulation medium.

Although the calibration procedure based on the electric stress determined by $\delta = 1/2$ is to some extent an approximation, it is the first time that the electric stress distribution factor in DC cable has been considered in cable space charge measurements. If a more precise charge distribution is required, δ values would need to be determined by a series of conductivity measurements.

5 Electric stress calculation

The method to determine the electric stress distribution across the cable insulation due to the external applied field and that as a consequence of the trapped charge in the bulk insulating material has been described in detail in an earlier paper [26]. Because of the limited spatial resolution in the space charge profile through the insulation, there are some errors introduced into the electric stress distribution calculations. Owing to the superposition of the large induced charge associated with the applied stress onto any relatively small amounts of accumulated charge close to the interfaces, the accuracy of the trapped charge density profile in the vicinity of the electrodes may be affected. Davies *et al* [27] proposed a method of calculation for the electric stress in planar samples to overcome the foregoing problems that can be applied to cable geometries.

The space charge profile with the external voltage removed after electrically ageing the cable sample at 80 kV for 60 minutes is shown in Fig. 5. The only charge present is that in the bulk and its image charges at the electrode interfaces. The magnitude of the charge density near the electrodes (o to d) and (o to $0'$) are not accurate because of the influence of the induced charge at electrode interface. However, over the region (d to c) the charge density profile is considered reasonable. The integration of the charge density over this region, expressed in (22), will give a correct electric stress distribution attributed purely by the presence of the space charge [25].

$$E(r) = \frac{1}{r\varepsilon_0\varepsilon_r} \int_c^d r\rho(r)dr + C \tag{22}$$

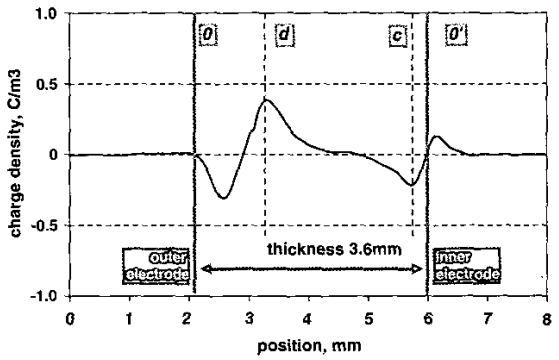

Fig. 5 *Charge density profile (with volts off)*

The electric stress E_a and E_b at the interfaces can be determined from the peak height of the output waveform [26]. Knowing the electric stresses at the interfaces and the stress in the middle of the sample and by extrapolating a line from c to E_a and d to E_b using a higher degree polynomial, the electric stress over the thickness ($0 \sim 0'$) of the cable sample can be mapped as shown in Fig. 6. The constant of integration C in (22) can be calculated from the 'equal energy' principle *i.e.* the area under the applied stress being equal to the one under the modified stress due to the presence of space charge in the bulk of the cable sample.

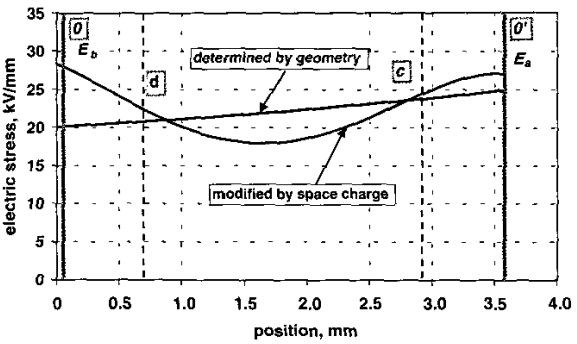

Fig. 6 *Calculation of electric stress distribution*

6 Results

Sample of XLPE cable with the inner and outer insulation radii 6.7 and 10.3 mm was subjected to electric stress and voltage reversal tests at ambient temperature. The designed operating stress of the sample under ac condition is about 10 kV/mm. The charge density and electric stress distributions for the different test conditions were determined from the PEA measurements.

The cable sample was initially subjected to a +80 kV direct voltage applied to the central conductor. In the experiment it was noticed that the charge generation slowed up after 80 minutes so the test was terminated after 90 minutes. The space charge distributions at different ageing times are shown in Fig. 7. Clearly, heterocharge has gradually accumulated close to the two electrodes with the charge build-up being larger near the outer electrode.

The voltage was then reversed with the negative polarity applied to the central conductor and the voltage ramped up to −80 kV within about 40 seconds to allow enough time to carry out the measurements at different voltages. Prior to the application of the negative voltage, the central conductor and the outer sheath was short-circuited for a short period of time for the release of the surface static charge.

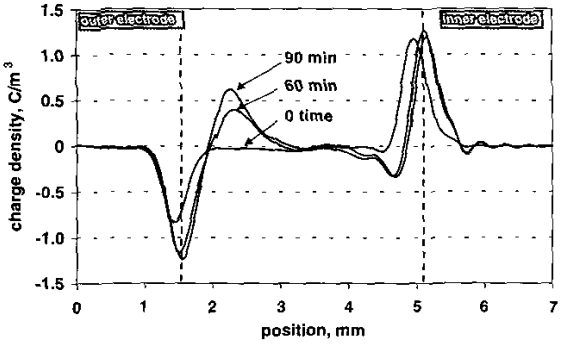

Fig. 7 *Space charge accumulation with ageing time (+80 kV at central conductor)*

The space charge response to the voltage polarity reversal and the voltage ramp is presented in Fig. 8 in which the accumulated charge, particularly the charge close to the outer electrode (peak ***b***), has not altered. As a result the induced charge at the outer electrode (peak ***a***) was significantly suppressed by this stable bulk charge. The observation was also made that, due to its relatively low magnitude and closeness to the inner electrode, the heterocharge was gradually neutralised by the newly formed heterocharge in the same region.

Over the period of 90 minutes at −80 kV the charge close to the outer electrode was slowly neutralised and a packet charge with similar magnitude but opposite sign was developed, as shown in Fig. 9. It is also noticed that the heterocharge near the inner electrode has built-up relatively quickly.

The formation of heterocharge in the cable is believed to be a result of the residual crosslinking byproducts. Under the influence of the applied electric stress, ionisation takes place with positive charge moving towards the cathode and negative charge towards the anode. It takes time to reach equilibrium due to the low mobility of the ionic charge. When the applied voltage is reversed, initially, the charge distribution in the bulk of the cable remains the same, and then is reduced due to the neutralisation of the existing

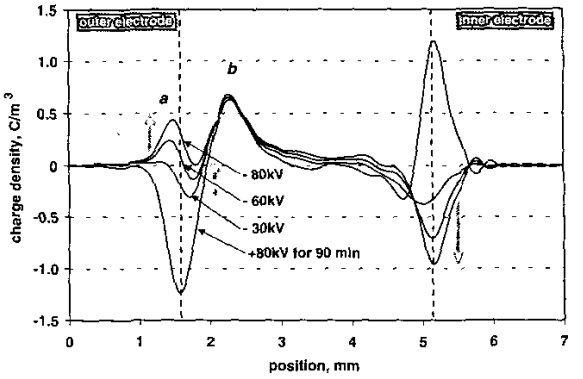

Fig. 8 *Space charge response to reversed applied voltage*

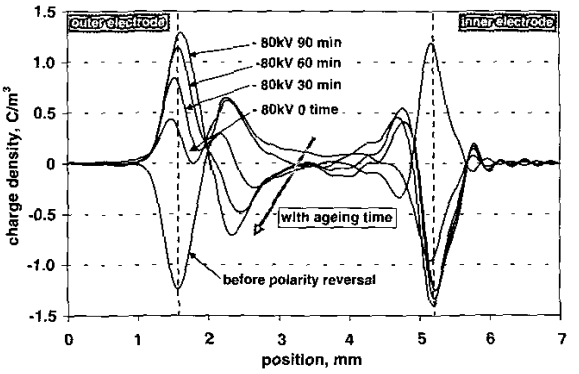

Fig. 9 *Space charge accumulation with reversed voltage application time*

charge with the newly formed charge. Finally, it reaches a new quasiequilibrium state under the applied voltage.

The electric stress distribution before and after the voltage polarity reversal was estimated using the method described in Section 5, and the results are plotted in Fig. 10.

Due to the presence of large heterocharge after 90 minutes of stressing at +80 kV, the interfacial stresses at the outer and inner interfaces have increased from its applied values 20.5 and 25.3 kV to 30.3 kV and 27.3 kV, respectively, noting that the stress at the outer sheath is higher than that at the inner electrode. On the other hand, the electric stress in the central region of the insulating material is reduced from ~22 to ~18 kV/mm.

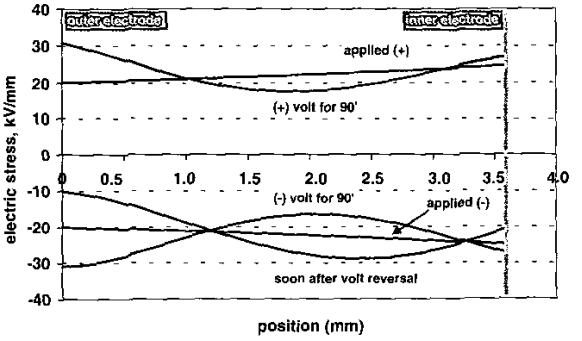

Fig. 10 *Electric stress distribution of 11 kV XLPE cable before and after voltage reversal*

When the external applied voltage is reversed, initially the electric stress in the central part of the insulation is significantly enhanced from ~18 to about −30 kV/mm because of the contribution of the previously accumulated space charge. This is the region where negative charge initiated and developed in the subsequent ageing period under the reversed voltage. After a certain period of stressing, the stress in this region reduces to −15 kV/mm due to the new heterocharge accumulation. Because of its slow response to the external voltage, the previously accumulated heterocharge in the voltage polarity reversal becomes a homocharge, thus the electric stress at the outer interface reduced from 30 to −10 kV/mm and from 27 to −20 kV/mm at the inner interface, respectively. After the stressing period with a negative voltage the interfacial stresses at the outer and inner electrode are enhanced to −30 and −27 kV/mm due to the build up of heterocharge which has a similar shape and magnitude but of opposite sign to that when a positive voltage applied.

It can be seen in Fig. 9 that the negative heterocharge, adjacent to the outer electrode, did not initiate from the region close to the interface, but from the central part of the cable insulation. This heterocharge moved towards the outer electrode with ageing time. This can be explained in terms of the electric stress enhancement in the central part of the insulating material after the voltage reversal due to the previously accumulated heterocharge. As noticed in Fig. 8, heterocharge generated under positive voltage is fairly stable and the charge variation or redistribution significantly lags behind the voltage change. As soon as the applied voltage was switched to negative, these charges will enhance the electric stress in the central part of the insulation, causing the reduction of interfacial stresses. The new packet charge (negative) initiated from the central material due to the higher stress started to neutralise the previously formed charge as it moved toward the outer electrode. In the mean time, the interfacial stress would also gradually increase because of new charge approaching from the centre of the insulation.

7 Conclusions

We have presented a technique using the PEA method to estimate the space charge and the electric stress distributions in polymeric insulated power cables operating under DC voltages. The modified PEA system has been introduced which adopts a flat ground electrode and makes the space charge measurement in the coaxial geometry cable samples much easier. By taking into account the divergence of the voltage pulse and the divergence of the acoustic wave (due to the cable geometry) across the insulation, and the attenuation/dispersion of the acoustic wave through the insulation, a more accurate space charge distribution has been obtained.

By way of a demonstration of the data processing methods developed, space charge measurements and the resultant electric stress profile for a commercial XLPE power cable under DC operating conditions have been presented. The sample was initially subjected to a positive polarity voltage at the central core, electrically stressed and then subjected to a negative polarity voltage. The space charge evolution over the stressing period shows satisfactory results in terms of accuracy in charge density and position resolution. The formation of heterocharge is believed to be associated with ionisation of the residues of the crosslinking byproducts. The electric stress distribution estimated from the space charge profiles show a significant effect of the voltage polarity reversal operation. The maximum electric stress can occur any where in the material in the combination of heterocharge formation and polarity reversal operation.

8 Dedication

It is sad that Prof. Tony Davies is no longer here to share our joy for the publication of the manuscript. Let the paper be dedicated to the memory of Prof. Tony Davies.

9 References

1 WATSON, P.K.: 'The transport and trapping of electrons in polymers', *IEEE Trans. Dielect. Electr. Insul.*, 1995, **2**, pp. 915–924
2 FUKUNAGA, K., MIYATA, H., TAKAHAASHI, T., YOSHIDA, S., and NIWA, T.: 'Measurement of space charge distribution in cable insulation using the pulsed electroacoustic method'. Proc. 3rd Int. Conf. on Polymer insulated power cables, Versailles, France, 23–27 June 1991, pp. 520–525
3 LIU, R., TAKADA, T., and TAKASU, N.: 'Pulsed electroacoustic method for measurement of charge distribution in power cables under both AC and DC electric field', *J. Phys. D Appl. Phys.*, 1993, **26**, pp. 986–993
4 HOZUMI, N., SUZUKI, H., OKAMOTO, T., WATANABE, K., and WATANABE, A.: 'Direct observation of time-dependent space charge profiles in XLPE cable under high electric fields', *IEEE Trans. Dielectr. Electr. Insul.*, 1994, **1**, pp. 1068–1076
5 FU, M., CHEN, G., DAVIES, A.E., and HEAD, J.: 'Space charge measurement in cables using the PEA method: -signal data processing considerations'. Proc. 7th Int. Conf. on Solid dielectrics, Eindhoven, Netherlands, 25–29 June 2001, pp. 219–222
6 TAKADA, T., and SAKAI, T.: 'Measurement of electric fields at a dielectric/electrode interface using an acoustic transducer technique', *IEEE Trans. Electr. Insul.*, 1983, **18**, pp. 619–628
7 MAENO, T., FUTAMI, T., KUSHIBE, H., TAKADA, T., and COOKE, C.M.: 'Measurement of spatial charge distribution in thick dielectrics using the pulsed electroacoustic method', *IEEE Trans. Electr. Insul.*, 1988, **23**, pp. 433–439
8 WANG, X., TU, D., TANAKA, Y., MURONAKA, T., TAKADA, T., SHINODA, C., and HASHZUMI, T.: 'Space charge in XLPE power cable under DC electrical stress and heat treatment', *IEEE Trans. Dielectr. Electr. Insul.*, 1995, **2**, pp. 467–474
9 LIM, F.N., FLEMING, R.J., and NAYBOUR, R.D.: 'Space charge accumulation in power cable XLPE insulation', *IEEE Trans. Dielectr. Electr. Insul.*, 1999, **6**, pp. 273–281
10 HOZUMI, N., TAKEDA, T., SUZUKI, H., and OKAMOTO, T.: 'Space charge behavior in XLPE cable insulation under 0.2–1.2 MV/cm DC fields', *IEEE Trans. Dielectr. Electr. Insul.*, 1998, **5**, pp. 82–90
11 TAKEDA, T., HOZUMI, N., FUJI, K., TERASHIMA, K., HARA, M., MURATA, Y., WATANABE, K., and YOSHIDA, M.: 'Space charge behavior in full-size 250 kV DC XLPE cables', *IEEE Trans. Power Deliv.*, 1998, **13**, pp. 28–39
12 FU, M., CHEN, G., DAVIES, D.E., TANAK, Y., and TAKADA, T.: 'A modified PEA space charge measurement system for power cables'. Proc. 6th Int. Conf. on Properties and applications of dielectric materials, Xian, China, 21–26 June 2000, pp. 104–107
13 DAVIES, A.E., CHEN, G., and VAZQUEZ, A.: 'Space charge measurement in dispersive dielectrics'. Proc. 5th Int. Conf. on Polymer insulated power cables, Versailles, 20–24 June 1999, pp. 733–738
14 MORSE, P.M., and INGARD, K.U.: 'Theoretical acoustics' (McGraw-Hill Book Co., NY, 1968)
15 BELTZER, A.I.: 'Acoustic of Solids' (Springer-Verlag, Berlin, Heidelberg, 1988)
16 BARNES, C.C.: 'Power Cables, Their Designs and Installation' (Chapman and Hall, London, UK, 1966)
17 WEEDY, B.M.: 'Electric Power System', 3rd Edn. (Wiley & Sons, Norwich, 1987)
18 WEEDY, B.M., and CHU, D.: 'HVDC extruded cables–parameters for determination of stress', *IEEE Trans. Power Appar. Syst.*, 1984, **103**, pp. 662–667
19 OUDIN, J.M., FALLOU, M., and THEVENON, H.: 'Design and development of DC cables', *IEEE Trans. Power Appar. Syst.*, 1967, **86**, pp. 304–311
20 BULLER, F.H.: 'Calculation of electrical stresses in dc cable insulation', *IEEE Trans. Power Appar. Syst.*, 1967, **86**, pp. 1169–1178
21 LIU, Z.: 'Electrical insulation design, -power cables' (Mechanic Industry Press (in Chinese) Beijing, China)
22 TANAKA, T., and GREENWOOD, A.: 'Advanced power cable technology, I' (CRC Press, USA, 1983)
23 MCALLISTER, I.W., CRICHTON, G.C., and PEDERSEN, A.: 'Charge accumulation in DC cable: a macroscopic approach'. Proc. of the 1994 IEEE Int. Symp. Electrical insulation, Pittsburgh, PA, USA, 5–8 June 1994, pp. 212–216

24 MCALLISTER, I.W., CRICHTON, G.C., and PEDERSEN, A.: 'Space charge field in DC cables'. Proc. of the 1996 IEEE Int. Symp. Electrical insulation, Montreal, Canada, 16–19 June 1996, pp. 661–665
25 FU, M.: 'Space charge measurement in polymer insulated power cables using the PEA method'. PhD Thesis, University of Southampton, UK 2002
26 FU, M., CHEN, G., DAVIES, A.E., and HEAD, J.: 'Space charge measurements in power cables using a modified PEA system'. Proc. 8th Int. Conf. on Dielectric materials, measurements and applications, Edinburgh, UK, 17–21 September 2000, pp. 74–79
27 DAVIES, A.E., CHEN, G., HAMPTON, N., SUTTON, S.J., and SWINGLER, G.: 'Calculation of charge density and electric stress in XLPE compounds'. Proc. 5th Int. Conf. on Polymer insulated power cables, Versailles, France, 20–24 June 1999, pp. 728–732